Revista de Metalurgia
October–December 2019, 55(4), e156
ISSN-L: 0034-8570
https://doi.org/10.3989/revmetalm.156

The effect of precipitation of metastable phases on the thermophysical and mechanical properties of the EN AW-6082 alloy

Uroš Stamenković✉, Svetlana Ivanov, Ivana Marković, Ljubiša Balanović, Milan Gorgievski

University of Belgrade, Technical Faculty in Bor, Vojske Jugoslavije 12, Bor, Serbia

(✉Corresponding author: ustamenkovic@tfbor.bg.ac.rs)

Submitted: 19 April 2019; Accepted: 20 November 2019; Available On-line: 20 December 2019

ABSTRACT: The effect of precipitation of metastable phases on the thermophysical and mechanical properties of the EN AW-6082 alloy was studied in this paper. After solid solution treatment and quenching in ice water samples were subjected to DSC analysis and thermal investigation with the aim to define optimal temperatures for isochronal annealing. Isochronal annealing was conducted at temperatures ranging from 160–330 °C for two annealing times – 30 and 60 minutes. Electrical conductivity, hardness, microhardness and structural properties were investigated during the isochronal aging treatment. Mechanical properties achieved peak values during aging at 230 °C for 30 minutes and at 220 °C for 60 minutes, respectively. Electrical conductivity gradually increased with an increase in aging temperature due to precipitation from the solid solution. Microstructural investigations by SEM-EDS confirmed the existence of precipitated phases and their distribution throughout the investigated samples.

KEYWORDS: Aging; Aluminum alloys; EN AW-6082; Heat treatment; Thermal properties

Citation/Citar como: Stamenković, U.; Ivanov, S.; Marković, I.; Balanović, L.; Gorgievski, M. (2019). "The effect of precipitation of metastable phases on the thermophysical and mechanical properties of the EN AW-6082 alloy". *Rev. Metal.* 55(4): e156. https://doi.org/10.3989/revmetalm.156

RESUMEN: *Efecto de la precipitación de fases metaestables en las propiedades termofísicas y mecánicas de la aleación EN AW-6082.* En este trabajo se estudia el efecto de la precipitación de fases metaestables sobre las propiedades termofísicas y mecánicas de la aleación EN AW-6082. Después del tratamiento con solución sólida y el enfriamiento rápido en agua helada, las muestras se sometieron a análisis DSC e investigación térmica con el objetivo de definir temperaturas óptimas para el recocido isocrónico. El recocido isocrónico se realizó a temperaturas que oscilan entre 160-330 °C durante dos tiempos de recocido: 30 y 60 min. La conductividad eléctrica, la dureza, la microdureza y las propiedades estructurales se investigaron durante el tratamiento de envejecimiento isocrónico. Las propiedades mecánicas alcanzaron valores máximos durante el envejecimiento a 230 °C durante 30 min y a 220 °C durante 60 min, respectivamente. La conductividad eléctrica aumentó gradualmente con un aumento en la temperatura de envejecimiento debido a la precipitación de la solución sólida. Las investigaciones microestructurales realizadas por SEM-EDS confirmaron la existencia de fases precipitadas y su distribución en todas las muestras investigadas.

PALABRAS-CLAVE: Aleaciones de aluminio; Envejecimiento; EN AW-6082; Propiedades térmicas; Tratamiento térmico

ORCID: Uroš Stamenković (https://orcid.org/0000-0002-7579-2159); Svetlana Ivanov (https://orcid.org/0000-0002-5326-0602); Ivana Marković (https://orcid.org/0000-0003-4431-9921); Ljubiša Balanović (https://orcid.org/0000-0002-3551-6731); Milan Gorgievski (https://orcid.org/0000-0002-9899-719X)

1. INTRODUCTION

Aluminium alloys from 6000 series are widely used in many applications due to excellent properties which can be additionally improved by precipitation hardening (Marioara *et al.*, 2001; Marioara *et al.*, 2003; Birol, 2006; Marioara *et al.*, 2006; Abid *et al.*, 2010; Birol, 2013; Prabhu, 2017; Acosta and Veleva, 2018). Alloys from this series are often used for production of heat sinks due to good electrical conductivity, high strength and good thermal properties (Karabay, 2006; Birol, 2013; Cui *et al.,* 2014; Choi *et al.*, 2014; Choi *et al.*, 2015; Kim *et al.*, 2018). The EN AW-6082 aluminium alloy is a good candidate for this application too. In the literature many research groups have investigated EN AW-6082 alloy and its properties during different parameters of heat. The increase in mechanical properties during different thermal treatments was studied by other authors (Gupta *et al.*, 2001; Marioara *et al.*, 2003; Birol, 2006; Abid *et al.*, 2010; Birol, 2013). Electrical conductivity change during aging treatment was studied by Birol (2013), Karabay (2006), and Cui *et al.* (2014). Prabhu (2017) reported the change in grain structure of the aged samples that provided the increase in hardness values of the 6082 aluminium alloy. Marioara *et al.* (2001), Marioara *et al.* (2003) and Marioara *et al.* (2006) followed the precipitation sequence by TEM analysis. The change in thermal properties was investigated by Choi *et al.* (2014), Choi *et al.* (2015), Zhang *et al.* (2016), Vishwakarma *et al.* (2017) and Kim *et al.* (2018). Kim *et al.* (2018) confirmed the highest thermal diffusivity at 250 °C for as-quenched samples. Choi *et al.* (2014) showed an increase in thermal conductivity and diffusivity of aged samples. Zhang *et al.* (2016) also proved that the thermal properties are highly influenced by the microstructure of the Al-Mg-Si-Cu alloy. Vishwakarma *et al.* (2017) defined the optimization model for obtaining the highest thermal properties for EN AW-6082 Al alloy. In review of the literature present, it can be concluded that aging process is defined primarily by aging temperature and time. The researches for EN AW-6082 alloy are based more on isothermal aging (Marioara *et al.*, 2001; Marioara *et al.*, 2003; Marioara *et al.*, 2006; Abid *et al.*, 2010; Cui *et al.*, 2014) rather than isochronal aging. Therefore, our aim was to investigate the influence of isochronal aging on thermophysical and mechanical properties of EN AW-6082. Optimal temperatures for isochronal annealing were defined by DSC analysis and thermal investigation. Our interests were focused on defining the isochronal aging regime that included short aging periods on higher temperatures which would try to yield the hardness values that are dictated by the European and American standards for these types of alloys and tempers (in this case T6 temper).

2. MATERIALS AND METHODS

For this experimental investigation an EN AW-6082 alloy was chosen. Extruded rectangular bars from "AlCu metali d.o.o." company were delivered in peak aged condition. Optical emission spectrometer "Belec Compact Port" was used for obtaining the chemical composition of the alloy, given in Table 1. O-temper was achieved by annealing the delivered samples at 550 °C for 6 hours in the electric resistance furnace Heraeus K-1150/2. After that, super saturated solid solution (α_{ssss}) was obtained by heat treatment at 550 °C for 1 hour and quenching in ice water. Quenched samples were subjected to isochronal aging at different temperatures, ranging from 160 °C to 330 °C for 30 minutes and 60 minutes. Mechanical and physical properties of the aged samples were compared to the quenched sample (noted as QS in Figures). The quenched sample was subjected to DSC analysis on SDT Q600 (TA Instruments) simultaneous DSC/TGA analyzer with heating rate of 10 °C·min^{-1} up to 600 °C. For investigating the thermophysical properties, Flash method was used with DXF 500 thermal analyzer manufactured by TA Instruments. Quenched samples were investigated by heating at the rate of 10 °C·min^{-1} in a nitrogen atmosphere. Electrical conductivity was measured using the electrical conductivity tester "Sigmatest 2.063". VEB Leipzig Vickers hardness tester with a 10 kg load and a 15 s dwelling time was used for hardness measurements. Additionally, microhardness values were measured using a PMT-3 Vickers microhardness tester using 100 gf loads with load duration of 15 s. The ASTM E384 standard was followed during both the hardness and microhardness measurements (ASTM E384-17, 2017).

TESCAN Vega 3 LMU scanning electron microscope equipped with an X act EDS detector by Oxford Instruments was used for metallographic phase investigations and distribution of phases.

3. RESULTS AND DISCUSSION

3.1. DSC analysis

The DSC thermogram of the quenched EN AW-6082 sample is shown in Fig. 1. The thermogram reveals the largely accepted precipitation sequence in

Table 1. Chemical composition of the investigated alloy (mass%)

Si	**Fe**	**Cu**	**Mn**	**Mg**	**Cr**	**Ni**	**Zn**
0.807	0.354	0.042	0.453	0.696	<0.012	0.012	0.115
Ti	**Pb**	**V**	**Co**	**Sn**	**Zr**	**Al**	
0.025	0.01	<0.003	0.006	<0.003	<0.003	97.45	

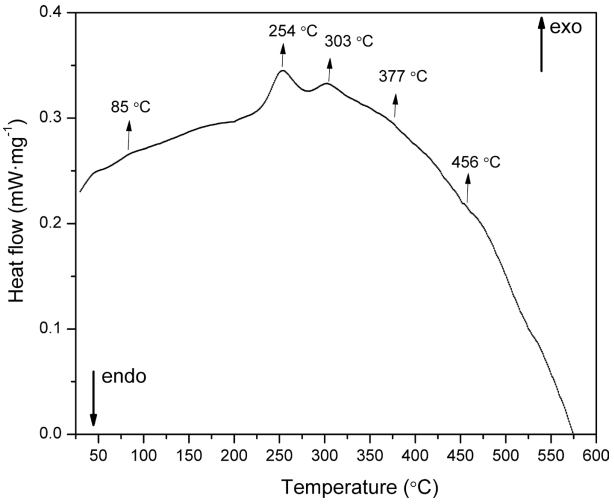

FIGURE 1. DSC curve of the EN AW-6082 investigated alloy.

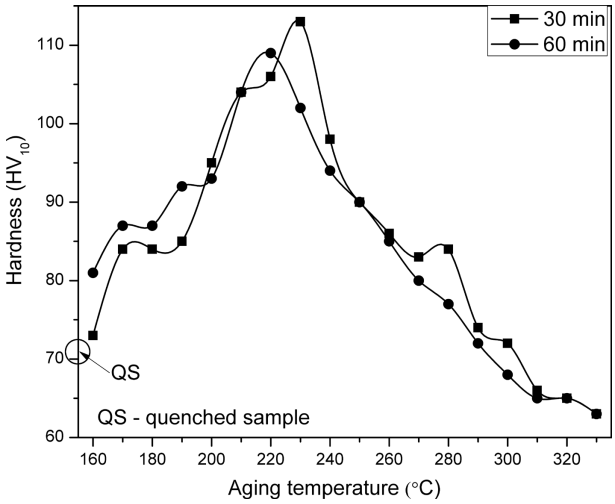

FIGURE 2. Hardness values of the EN AW-6082 alloy after the isochronal aging treatment.

Al-Mg-Si alloys which is well established to be SSSS (super saturated solid solution)→ atomic clusters→ G.P. zones→ β''→ β'→ Si (if there is excess silicon in alloys composition)→ β (Zhen *et al.*, 1997; Edwards *et al.*, 1998; Gupta *et al.*, 2001; Vedani *et al.*, 2007; Shang *et al.*, 2011; Birol, 2013; Kim *et al.*, 2018). It can be seen from Fig. 1 that five exothermic peaks appear in Fig. 1. Some of these peaks are less pronounced and this can be attributed to the low calorimetric effect (Zhen *et al.*, 1997). The first exothermic peak appears at around 85 °C and it is associated with the Mg:Si clustering (Edwards *et al.*, 1998; Birol, 2006). The two exothermic peaks with their maximums situated at 254 °C and 303 °C represent the formation of metastable β'' and β' precipitates, respectively (Zhen *et al.*, 1997; Edwards *et al.*, 1998; Birol, 2006; Vedani *et al.*, 2007; Abid *et al.*, 2010; Shang *et al.*, 2011; Birol, 2013; Choi *et al.*, 2015; Kim *et al.*, 2018). In the literature many researchers study the effect of metastable β'' phase on different properties. According to Marioara *et al.* (2001), it's a needle-like phase with monoclinic lattice with the unit cell parameters, a = 15.16 Å, b = 4.05 Å, c = 6.74 Å, β = 105.3° that precipitates along the <100> Al direction. Also, depending on the aging parameters, β'' phase is often very finely dispersed throughout the structure, reaching the 100.000 – 200.000 particles per square micrometer (Marioara *et al.*, 2003). The precipitation of the excess Si and the formation of the equilibrium β phase is represented by the last two exothermic peaks appearing at 377 °C and 456 °C (Birol, 2013).

3.2. Investigation of mechanical properties

Figure 2 shows the development of absolute hardness change as a function of annealing temperature at two different aging times. Hardness gradually increases with aging temperature and it reaches maximum value at 230 °C, when aged for 30 minutes. This peak is in agreement with the DSC analysis as it represents the precipitation of the metastable β'' phase, which is mainly responsible for the high hardness values (Marioara *et al.*, 2001; Gupta *et al.*, 2001; Abid *et al.*, 2010; Birol, 2013). In comparison with the hardness of 71 HV10 for the quenched sample (circled out in the graph), the peak aged sample has a hardness value of 113 HV10 when aged for 30 minutes and 109 HV10 when aged for 60 minutes. That's a 59.15% increase for the sample aged at 230 °C for 30 minutes, and a 53.52% increase for the sample aged at 220 °C for 60 minutes. Peak aged samples, at both aging times, reached the hardness values that are recommended by the standard EN 755-2:2016 (EN 755-2, 2016). As aging temperature increases the hardness values decrease due to the transformation of the metastable β'' hardening phase. The formation of β' metastable phases can increase the hardness values but only by a small amount, as seen in Fig. 2 at the temperatures between 260–300 °C. By comparing the two graphs presented in Fig. 2, it can be seen that aging for longer time shifts the peak for maximum hardness to the lower temperatures. All the other peaks, after the peak aged state, are more pronounced when aged for a shorter time.

The same conclusions were also drawn by measuring the microhardness of the investigated samples, as shown in Fig. 3. Peak microhardness due to precipitation of β'' phase was achieved at 230 °C when aged for 30 minutes with a 44.6% increase in microhardness value, in relation to the quenched sample, from 94 HV0.1 to 136 HV0.1. When aged for 60 minutes at 220 °C there was a 38.29% increase in microhardness value, again in relation to the quenched sample, from 94 HV0.1 to 130 HV0.1. After the aging at higher temperature

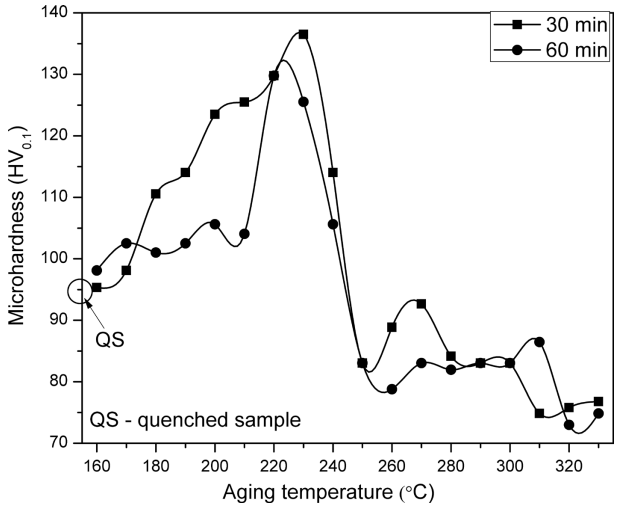

FIGURE 3. Microhardness values of the EN AW-6082 alloy after the isochronal aging treatment.

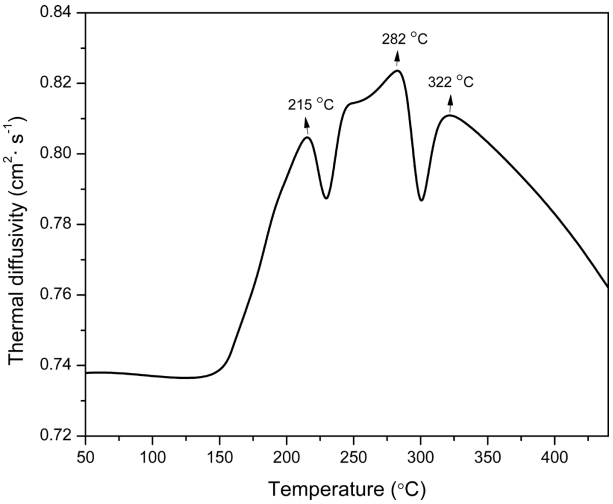

FIGURE 4. Electrical conductivity values of the EN AW-6082 alloy after the isochronal aging treatment.

than 230 °C the microhardness values rapidly decrease due to overaging.

3.3. Investigation of electrical conductivity

Figure 4 shows the effect of aging temperature on the electrical conductivity values of the investigated alloy. In Al-Mg-Si alloys there is a strong connection between electrical conductivity and precipitation, so measuring this property can be well used for investigation of the precipitation processes (Karabay, 2006). There is a sudden drop in electrical conductivity for aged samples compared to the quenched one. The electrical conductivity for the quenched sample is 28 MS/m and it decreases after aging at 160 °C. This drop can be explained via the formation of clusters, closely spaced GP zones and fine early-stage precipitates, which both carry the strong electron scattering effect, mentioned by some researchers (Edwards *et al.*, 1998; Cui *et al.*, 2014; Prabhu, 2017). After the initial drop, there is a gradual increase in electrical conductivity values as aging continues, and clusters and early-stage precipitates coarsen due to diffusion process. After aging at higher temperatures than 210 °C for both aging times, samples exceed the electrical conductivity values of the quenched one. As the matrix gets less saturated (loses all the quenched-in elements) during the aging treatment, as a result of the formation of metastable β'' and β' phases, the electrical conductivity increases (Karabay, 2006; Cui *et al.*, 2014). It can be observed that the 60 minutes aging curve is slightly higher than the 30 minutes aging curve. This can be associated with the easier formation of pre-β'' and β'' phases due to the prolonged aging time, as confirmed by Cui *et al.* (2014).

3.4. Investigation of thermal properties

Thermal diffusivity, conductivity and specific heat of the quenched samples were investigated during the continuous heating in Figs. 5–7, respectively. It is expected that the thermal diffusivity and conductivity decrease with the increase in temperature due to heat vibrations of the atoms and the interruption of electron movement (Tritt, 2004). However, there are increases in these properties during the continuous heating during which the precipitation sequence takes place (Kim *et al.*, 2018). In the 200–220 °C temperature range the first peak appears for all measured thermal properties due to formation of pre-β'' phase. As the temperature rises, precipitation continues and the values of

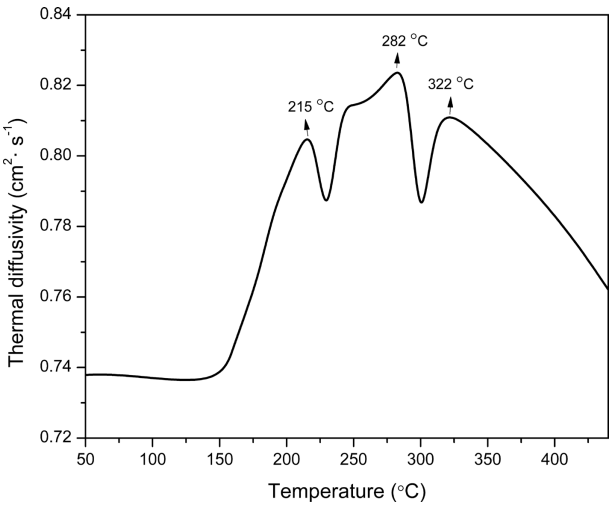

FIGURE 5. Thermal diffusivity of quenched EN AW-6082 alloy during the continuous heating.

thermal diffusivity, conductivity and heat capacity rise. Two more peaks appear at around 280 °C and 320 °C due to formation of the β'' and β' phases, respectively. Thermal properties have highest values at these peaks due to the reduction of alloying elements in the solid solution caused by the precipitation (Kim *et al.*, 2018; Choi *et al.*, 2019). The peaks for maximal values of hardness and electrical conductivity partially coincide with the peaks obtained for thermal properties. However, the obtained curves for thermal properties shift to the right side of the diagram due to continuous heating and measuring equipment. The specific heat of the investigated alloy increases monotonically with temperature; however, it is not as much influenced by the precipitation of phases that appear in the investigated temperature range comparatively to thermal diffusivity and conductivity measurements (Choi *et al.*, 2015).

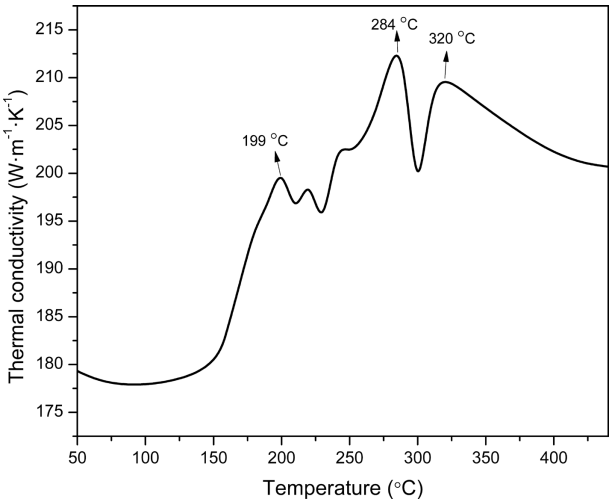

FIGURE 6. Thermal conductivity of quenched EN AW-6082 alloy during the continuous heating.

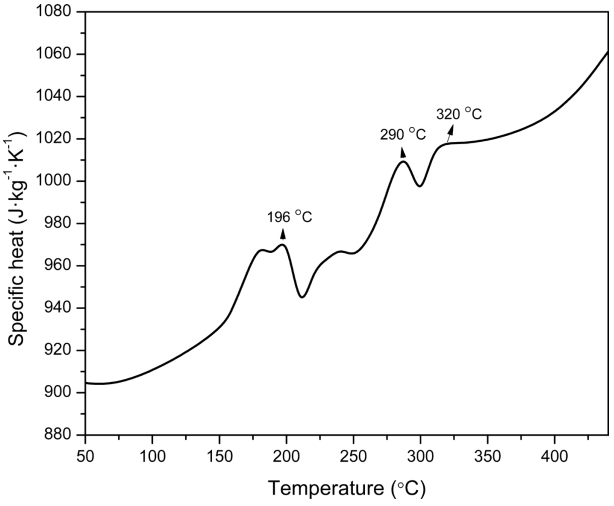

FIGURE 7. Thermal conductivity of quenched EN AW-6082 alloy during the continuous heating.

3.5. Microstructural investigation

In order to complete the investigation in more detail and study the structural change of the aging process, SEM-EDS analyses were performed. Aged samples with minimal and maximal hardness values were chosen for microstructural investigation i.e. samples aged at 160 °C and 220/230 °C for 30 minutes and 60 minutes. Figure 8 shows the microstructures of the aged samples in different aging conditions. It can be seen that the amount of metastable phases increases with an increase in temperature and aging time.

To further investigate the aforementioned phases, EDS analysis was performed on the sample with the highest hardness value (after aging at 230 °C for 30 minutes), as presented in Fig. 9 and Table 2. In the aged samples, almost the entire structure is covered with finely dispersed particles of the metastable β'' phase, represented by the spectrum 5 in Fig. 9. Some authors suggested that the ideal ratio of the magnesium and silicon in β'' phase should be 5 to 6 (Marioara *et al.*, 2003; Marioara *et al.*, 2006).

Our result doesn't confirm this suggestion probably due to excess Si; still it can be assumed that β'' phase does appear as finely dispersed. Ultra-fine particles of this phase are very hard to detect at these magnifications; however hardness and microhardness

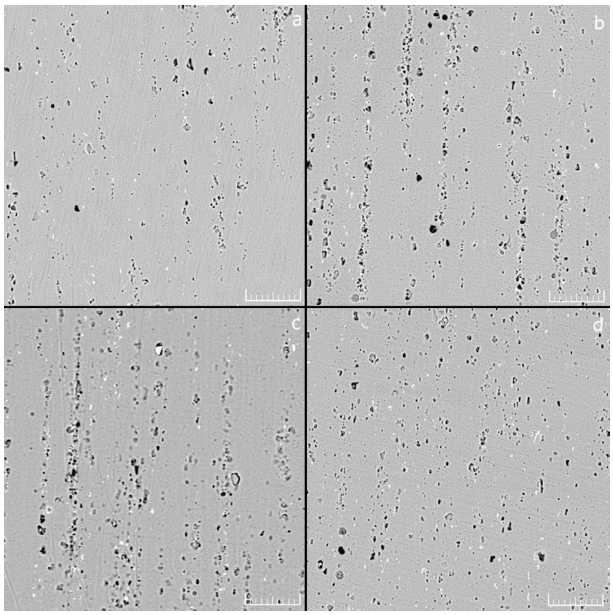

FIGURE 8. SEM microstructures of investigated alloy after different aging treatment: a) aged at 160 °C for 30 minutes; b) aged at 230 °C for 30 minutes; c) aged at 160 °C for 60 minutes; d) aged at 220 °C for 60 minutes; magnification bar is 50 μm.

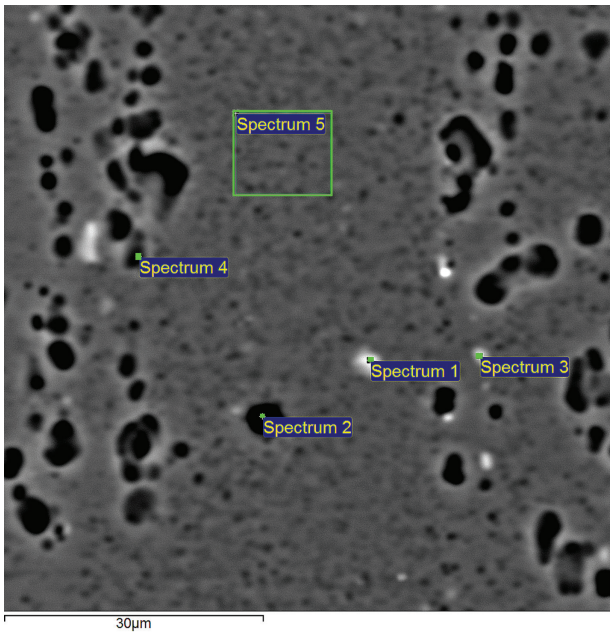

FIGURE 9. SEM and EDS analyses of EN AW-6082 alloy after aging at 230 °C for 30 minutes.

TABLE 2. Chemical composition of the analyzed spectrums (at. %)

Spectrum	Mg	Al	Si	Mn	Fe
Spectrum 1		83	6.33	3.19	7.51
Spectrum 2	0.42	99.2	0.23	0.19	–
Spectrum 3	0.5	92	3.25	1.51	2.71
Spectrum 4	0.58	98.2	1.09	0.13	–
Spectrum 5	0.61	98.2	1.02	0.14	–

results obtained for the sample aged at 230 °C for 30 minutes indirectly show its existence. In the investigated sample, there is a phase that appears light grey to white in colour. This phase is the quaternary AlMnFeSi phase, represented by spectrums 1 and 3. There is also an additional phase that appears as dark particles throughout the structure. This phase is also a quaternary phase but based on Al, Mg, Mn, Si as presented on spectrums 2 and 4.

4. CONCLUSIONS

Achievements in this paper can be summarized as follows:

- The DSC analysis revealed the largely accepted precipitation sequence with the presence of exothermic peaks due to the formation of metastable/stable phases.
- Hardness and microhardness values significantly increase during isochronal aging due to the formation of the metastable β'' phase. At both aging times, peak aged samples reached the hardness values that are recommended by the European norm standard for T6 temper. After aging at 230 °C for 30 minutes, hardness increased 59.15% and microhardness 44.6%; while aging at 220 °C for 60 minutes generated 53.52% increase in hardness values and 38.29% increase in microhardness values when compared to quenched sample.
- After an initial drop in electrical conductivity, a gradual increase was detected after isochronal aging treatment. The increase in electrical conductivity was detected due to the formation of metastable β'' and β' phases which caused matrix to get less saturated. Electrical conductivity was increased by 16.07% after aging at 290 °C for 30 minutes, and by 16.78% after aging at 330 °C for 60 minutes when compared to the quenched sample.
- Thermal diffusivity, conductivity and specific heat are influenced by the precipitation sequence and are in accordance with the DSC thermogram and precipitation sequence. Also, it is confirmed that these properties can be further used as a tool for investigating the aging in these types of alloys.
- Microstructural investigation showed the existence of hardening phases that were responsible for the increment of physical, thermal and mechanical properties.

ACKNOWLEDGMENTS

The research results were developed with the assistance of the Ministry of Education, Science and Technological Development of the Republic of Serbia under the projects OI 172037 and TR34003.

REFERENCES

Abid, T., Boubertakh, A., Hamamda, S. (2010). Effect of pre-aging and maturing on the precipitation hardening of an Al–Mg–Si alloy. *J. Alloys Compd.* 490 (1–2), 166–169. https://doi.org/10.1016/j.jallcom.2009.10.096.

Acosta, G., Veleva, L. (2018). Mapping initial stages of localized corrosion of AA6061-T6 in diluted substitute ocean water by LEIS and SKP. *Rev. Metal.* 54 (4), e134. https://doi.org/10.3989/revmetalm.134.

ASTM E384-17 (2017). Standard Test Method for Microindentation Hardness of Materials, ASTM Intenational, West Conshohocken, PA, USA.

Birol, Y. (2006). The effect of processing and Mn content on the T5 and T6 properties of AA6082 profiles. *J. Mater. Process. Tech.* 173 (1), 84–91. https://doi.org/10.1016/j.jmatprotec.2005.09.029.

Birol, Y. (2013). Precipitation during homogenization cooling in AlMgSi alloys. *Trans. Nonferr. Metal. Soc. China* 23 (7), 1875–1881. https://doi.org/10.1016/S1003-6326(13)62672-2.

Choi, S.W., Kim, Y.M., Lee, K.M., Cho, H.S., Hong, S.K., Kim, Y.C., Kang, C.S., Kumai, S. (2014). The effects of cooling rate and heat treatment on mechanical and thermal characteristics of Al–Si–Cu–Mg foundry alloys. *J. Alloys*

Compd. 617, 654–659. https://doi.org/10.1016/j.jallcom.2014.08.033.

Choi, S.W., Cho, H.S., Kang, C.S., Kumai, S. (2015). Precipitation dependence of thermal properties for Al–Si–Mg–Cu–(Ti) alloy with various heat treatment. *J. Alloys Compd.* 647, 1091–1097. https://doi.org/10.1016/j.jallcom.2015.05.201.

Choi, S.W., Kim, Y.M., Kim, Y.C. (2019). Influence of precipitation on thermal diffusivity of Al-6Si-0.4Mg-0.9Cu-(Ti) alloys. *J. Alloys Compd.* 775, 132–137. https://doi.org/10.1016/j.jallcom.2018.10.068.

Cui, L., Liu, Z., Zhao, X., Tang, J., Liu, K., Liu, X., Qian, C. (2014). Precipitation of metastable phases and its effect on electrical resistivity of Al-0.96Mg2Si alloy during aging. *Trans. Nonferr. Metal. Soc. China* 24 (7), 2266–2274. https://doi.org/10.1016/S1003-6326(14)63343-4.

Edwards, G.A., Stiller, K., Dunlop, G.L., Couper, M.J. (1998). The precipitation sequence in Al–Mg–Si alloys. *Acta Mater.* 46 (11), 3893–3904. https://doi.org/10.1016/S1359-6454(98)00059-7.

EN 755-2 (2016). Aluminium and aluminium alloy - Extruded rod/bar, tube and profiles. European Committee for Standardization.

Gupta, A.K., Lloyd, D.J., Court, S.A. (2001). Precipitation hardening in Al–Mg–Si alloys with and without excess Si. *Mat. Sci. Eng. A* 316 (1–2), 11–17. https://doi.org/10.1016/S0921-5093(01)01247-3.

Karabay, S. (2006). Modification of AA-6201 alloy for manufacturing of high conductivity and extra high conductivity wires with property of high tensile stress after artificial aging heat treatment for all-aluminium alloy conductors. *Mater. Design* 27 (10), 821–832. https://doi.org/10.1016/j.matdes.2005.06.005.

Kim, Y.M., Choi, S.W., Kim, Y.C., Kang, C.S., Hong, S.K. (2018). Influence of the Precipitation of Secondary Phase on the Thermal Diffusivity Change of Al-Mg_2Si Alloys. *Appl. Sci.* 8 (11), 2039. https://doi.org/10.3390/app8112039.

Marioara, C.D., Andersen, S.J., Jansen, J., Zandbergen, H.W. (2001). Atomic model for GP-zones in a 6082 Al–Mg–Si system. *Acta Mater.* 49 (2), 321–328. https://doi.org/10.1016/S1359-6454(00)00302-5.

Marioara, C.D., Andersen, S.J., Jansen, J., Zandbergen, H.W. (2003). The influence of temperature and storage time at RT on nucleation of the β" phase in a 6082 Al–Mg–Si alloy. *Acta Mater.* 51 (3), 789–796. https://doi.org/10.1016/S1359-6454(02)00470-6.

Marioara, C.D., Nordmark, H., Andersen, S.J., Holmestad, R. (2006). Post-β" phases and their influence on microstructure and hardness in 6xxx Al-Mg-Si alloys. *J. Mater. Sci.* 41 (2), 471–478. https://doi.org/10.1007/s10853-005-2470-1.

Prabhu, T.R. (2017). Effects of ageing time on the mechanical and conductivity properties for various round bar diameters of AA 2219 Al alloy. *Eng. Sci. Technol. Int. J.* 20 (1), 133–142. https://doi.org/10.1016/j.jestch.2016.06.003.

Shang, B.C., Yin, Z.M., Wang, G., Liu, B., Huang, Z.Q. (2011). Investigation of quench sensitivity and transformation kinetics during isothermal treatment in 6082 aluminum alloy. *Mater. Design* 32 (7), 3818–3822. https://doi.org/10.1016/j.matdes.2011.03.016.

Tritt, T.M. (2004). *Thermal Conductivity: Theory, Properties and Applications*. Kluwer Academic/ Plenum Publisher, New York.

Vedani, M., Angella, G., Bassani, P., Ripamonti, D., Tuissi, A. (2007). DSC analysis of strengthening precipitates in ultrafine Al–Mg–Si alloys. *J. Therm. Anal. Calorim.* 87 (1), 277–284. https://doi.org/10.1007/s10973-006-7837-2.

Vishwakarma, D.K., Kumar, N., Padap, A.K. (2017). Modelling and optimization of aging parameters for thermal properties of Al 6082 alloy using response surface methodology. *Mater. Res. Express* 4 (4), 046502. https://doi.org/10.1088/2053-1591/aa68c1.

Zhang, C., Du, Y., Liu, S, Liu, Y., Sundman, B. (2016). Thermal conductivity of Al–Cu–Mg–Si alloys: Experimental measurement and CALPHAD modeling. *Thermochim. Acta* 635, 8–16. https://doi.org/10.1016/j.tca.2016.04.019.

Zhen, L., Fei, W.D., Kang, S.B., Kim, H.W. (1997). Precipitation behaviour of Al-Mg-Si alloys with high silicon content. *J. Mater. Sci.* 32 (7), 1895–1902. https://doi.org/10.1023/A:1018569226499.